

Pressure-Induced Magnetic Transition in Manganite ($\text{La}_{0.75}\text{Ca}_{0.25}\text{MnO}_3$)

Yang Ding,^{1,*} Daniel Haskel,² Yuan-Chieh Tseng,^{2,3} Eiji Kaneshita,² Michel van Veenendaal,^{2,4} J. F. Mitchell,⁵ Stanislav V. Sinogeikin,⁶ Vitali Prakapenka,⁷ and Ho-kwang Mao^{1,6,8}

¹HPSynC, Carnegie Institution of Washington, 9700 South Cass Avenue, Argonne, Illinois 60439, USA

²Advanced Photon Source, Argonne National Laboratory, Argonne, Illinois 60439, USA

³Department of Materials Science and Engineering, Northwestern University, Evanston, Illinois 60201, USA

⁴Department of Physics, Northern Illinois University, De Kalb, Illinois 60115, USA

⁵Materials Science Division, Argonne National Laboratory, Argonne, Illinois 60439, USA

⁶HPCAT, Carnegie Institution of Washington, Building 434E, 9700 South Cass Avenue, Argonne, Illinois 60439, USA

⁷GSECARS, University of Chicago, Advanced Photon Source, Building 434A, 9700 South Cass Avenue, Argonne, Illinois 60439, USA

⁸Geophysical Laboratory, Carnegie Institution of Washington, 5251 Broad Branch Road, N.W., Washington, D.C. 20015, USA

(Received 30 July 2008; revised manuscript received 29 January 2009; published 10 June 2009)

Low temperature Mn *K*-edge x-ray magnetic circular dichroism and x-ray diffraction measurements were carried out to investigate the stability of the ferromagnetic ground state in manganite $\text{La}_{0.75}\text{Ca}_{0.25}\text{MnO}_3$ under nearly uniform compression using diamond anvil cells. The magnetic dichroism signal gradually decreases with pressure and disappears at 23 GPa, and meanwhile a uniaxial compression of MnO_6 octahedra along the *b* axis is observed to continuously increase with pressure and become anomalously large at 23.5 GPa. These changes are attributed to a ferromagnetic-antiferromagnetic transition that is associated with orbital ordering at high pressure.

DOI: 10.1103/PhysRevLett.102.237201

PACS numbers: 75.30.-m, 62.50.-p, 75.50.-y, 78.70.Dm

Pseudocubic perovskite-type manganites have received renewed interest since the discovery of the colossal magnetoresistance phenomenon [1]. However, a complete understanding of the physics underlying manganite properties at the microscopic level has not yet been achieved, mainly due to the complexity arising from the competition between double exchange and superexchange, as well as the interplay between magnetic ordering, orbital ordering, and Jahn-Teller effect [2–6]. The multitude of competing ground states can be tuned or manipulated with external stimuli, such as temperature and pressure, and electric or magnetic fields. Among these, the effect of pressure still remains unclear.

Recently, theories have suggested that the decrease in Curie temperature (T_c) and insulator-metal transition temperature (T_{IM}) with pressure [7] may originate in the increase of the strength of superexchange-mediated AFM interactions among t_{2g} electrons [8]. Accordingly, a FM-AFM transition could possibly be induced at higher pressures, motivating our study in an extended pressure range using high-pressure x-ray magnetic circular dichroism (XMCD) [9–11] and x-ray diffraction experiments. In this Letter we report on the stability of the magnetic ground state of $\text{La}_{0.75}\text{Ca}_{0.25}\text{MnO}_3$ up to 27 GPa at low temperature, significantly extending the pressure range beyond that of previous studies [12–17]. We observe that the ferromagnetic state becomes unstable with pressure and disappears at 23 GPa, a transition that is correlated with a uniaxial compression of MnO_6 octahedra along the *b* axis. These changes are attributed to a transition from an orbitally disordered, *F*-type FM phase to an or-

bitally ordered, *A*-type AFM state, which arises from the preferential occupation of e_g x^2-y^2 orbitals over $3z^2-r^2$ orbitals upon compression.

The XMCD measurements were performed at undulator beam line 4-ID-D of the Advanced Photon Source (APS), Argonne National Laboratory [18]. The method of the sample's synthesis is similar to that given in Ref. [19]. Samples were finely ground and mixed with silicon oil pressure-transmitting medium then loaded into a piston-cylinder membrane-driven CuBe cell with perforated diamond anvils [18]. Pressure was calibrated using the fluorescence shift of ruby powders loaded with the sample, accounting for temperature correction [20]. In the experiments, the energy of the incident x-ray beam was scanned through the Mn *K* absorption edge (6539 eV) to acquire both the x-ray absorption near edge structure (XANES) and XMCD spectra. Data were collected between 2.0 and 23.0 GPa at 13 K in a $H = 0.6$ T applied field. The x-ray powder diffraction experiments were conducted at sector 16-ID-B station of the HPCAT sector, Advanced Photon Source, Argonne National Laboratory, using a monochromatic beam ($E = 30.43$ keV). Fine powder samples were loaded with ruby pressure standard and helium pressure medium in a Mao-type symmetric diamond anvil cell, which is loaded in a cryogenic stage that provided a minimum temperature of 40 K. The diffraction patterns were collected using a MAR165 CCD (pixel size $79 \times 79 \mu\text{m}^2$), and the exposure time was typically from 600–1200 s. FIT2D [21] and GSAS [22] programs were used to process and fit the diffraction data, respectively.

Figure 1 shows normalized XANES and XMCD spectra collected at 2.0 and 23.0 GPa, respectively. Line shapes of spectra are in good agreement with previously reported Mn K -edge data on a similar compound ($\text{La}_{0.67}\text{Ca}_{0.33}\text{MnO}_3$) at ambient conditions [23]. Figure 2 shows pressure dependent XMCD data. The strength of XMCD decreases monotonically with pressure and becomes indistinguishable from the noise at ~ 23 GPa, as seen in the plot of integrated XMCD intensity in Fig. 2. It is generally accepted that the spin polarization of $4p$ states probed in the K -edge dipole transition arises predominantly from onsite and intersite exchange interactions with polarized $3d$ states [24–30], and therefore, changes in $3d$ polarization directly affect the K -edge XMCD. Even though the XMCD magneto-optical sum rule for the K edge only relates to the expectation value of the orbital angular momentum per $4p$ hole [30], it is reasonable to argue that the overall strength of Mn K -edge XMCD should be proportional to the ordered, net $3d$ magnetic moment of the sample. The reduction in the K -edge XMCD of Mn sites indicates that this ordered FM moment decreases with pressure, to vanish at ~ 23 GPa where the XMCD signal and long-range FM ordering disappears. We note that changes in the intersite, $3d$ - $4p$ hybridization alone cannot explain the reduction in XMCD since such hybridization is expected to increase with pressure and would have resulted in an increase of the XMCD signal in the absence of a reduction in the ordered FM $3d$ moment. Upon pressure release the XMCD signal recovers to its corresponding strength at ambient pressure (Fig. 2) indicating that the magnetic transition is reversible.

Figure 3 shows the diffraction results collected between 13.0 to 26.9 GPa, at $T = 40$ K. The structural refinements indicate that $\text{La}_{0.75}\text{Ca}_{0.25}\text{MnO}_3$ retains its $Pnma$ perovskite structure within the investigated P - T range, and no discontinuity is observed in the P - V curve (Fig. 3). However, an anomalous change in lattice strain and Mn-O₁/Mn-O₂ bond-length ratio was observed at 23.5 GPa, as shown in Figs. 3(b), a similar P - T condition at which the XMCD

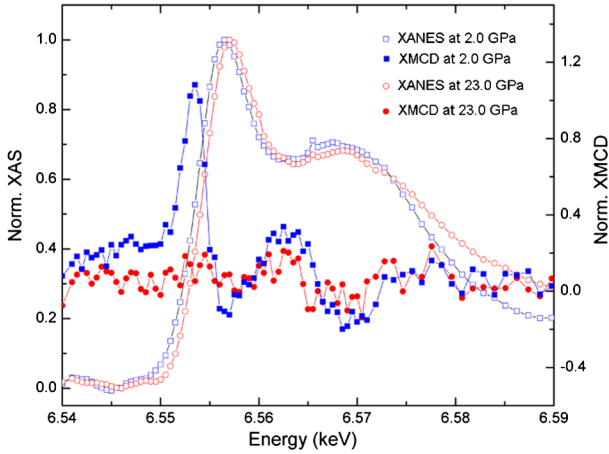


FIG. 1 (color online). Normalized XANES and XMCD data for $\text{La}_{0.75}\text{Ca}_{0.25}\text{MnO}_3$ at 13 K collected at 2.0 and 23.0 GPa. The XMCD peak intensity is about 0.1% of the absorption jump.

signal disappears. This indicates the magnetic transition is correlated with a structural change. Though XMCD alone does not unambiguously demonstrate that the zero-net moment state displays AFM ordering, the concomitant structural changes revealed from diffraction measurements provide important clues to decipher the magnetic state above 23 GPa, as discussed below.

The magnetic ordering within the MnO_2 plane (or ac lattice plane) and between MnO_2 planes (along b axis) is determined by the competition between the AFM superexchange between the core t_{2g} electrons and FM double exchange through the itinerant e_g electrons. The strength of double exchange in the MnO_2 plane or between the planes depends on the occupancy of the e_g orbitals because of anisotropic hopping, which is affected by the amount of strain in MnO_6 octahedra [31]. It is known that the ground state of $\text{La}_{0.75}\text{Ca}_{0.25}\text{MnO}_3$ is stable in an F -type FM structure with a negligible lattice strain below the Curie temperature at ambient pressure, and no orbital ordering has been observed so far. This suggests that the two e_g orbitals (x^2-y^2 and $3z^2-r^2$) remain nearly degenerate and equally populated [32].

However, with increasing pressure, a uniaxial compression of the MnO_6 octahedra along axis b is observed. The strain for the distortion can be measured from three pairs of nonequivalent Mn–O bonds in MnO_6 octahedra: Mn–O₁, along the b axis, and two Mn–O₂ bonds within the ac plane (Fig. 4). At high pressures, the strain increases. It reaches 2.3% at 13.0 GPa, 3.9% 23.5 GPa, and 6.1% at 27.0 GPa, respectively, as shown in Fig. 3(b). With such a large strain in MnO_6 , the Mn– e_g orbitals are no longer degenerate. The significant contraction of the Mn–O₁ distance raises the energy of $3z^2-r^2$ orbitals relative to that of x^2-y^2 orbitals

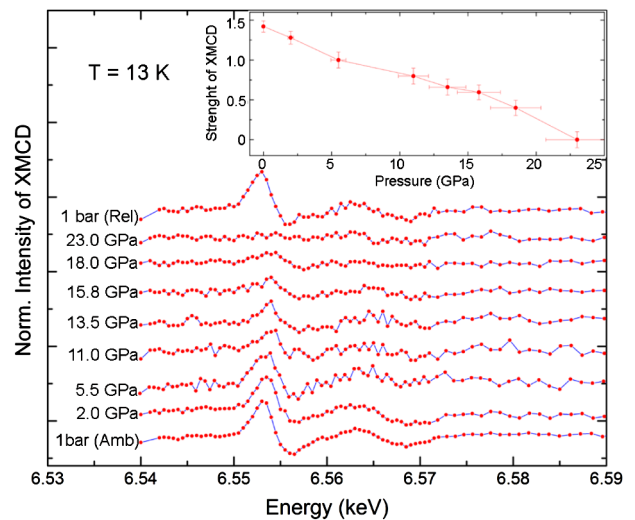


FIG. 2 (color online). Normalized XMCD data of manganite $\text{La}_{0.75}\text{Ca}_{0.25}\text{MnO}_3$ collected at 13 K from 1 bar to 23.0 GPa. The inset shows the intensity of overall XMCD strength versus pressure. [“1 bar (Rel)” is taken after pressure release; “1 bar (Amb)” is taken at ambient conditions].

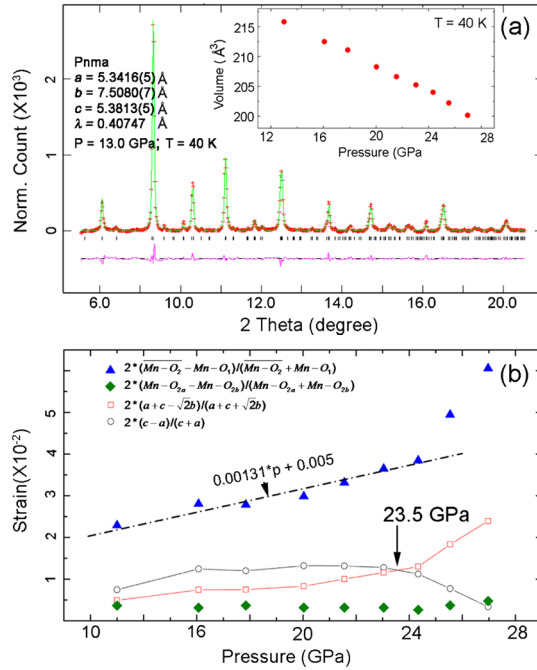


FIG. 3 (color online). (a) Structure refinement of diffraction patterns at 13.0 GPa 40 K with the program GSAS; (cross: measured pattern; line: calculated pattern; black tick: position of peaks; line below tick: difference between calculated and measured patterns). The inset is a plot of pressure versus volume. (b) The strain for lattice and MnO_6 octahedral versus pressure. (For $Pnma$, we set lattice parameter as $b > c > a$.) The dashed line is an estimated pressure dependence of strain, equal to $0.00131 \times P + 0.005$. $Mn-O_1$ and $Mn-O_{2a}$, $Mn-O_{2b}$ represent the bond length. The $Mn-O_2$ bond length is averaged from $Mn-O_{2a}$ and $Mn-O_{2b}$ bond length within the ac plane (Fig. 4).

and a change in the angular distribution of e_g electrons ensues, the e_g electrons preferentially occupying x^2-y^2 orbitals. As a result, the e_g electrons in x^2-y^2 orbitals enhance the double exchange within the MnO_2 planes favoring FM ordering. In contrast, as the $3z^2-r^2$ orbitals become unoccupied, the coupling between MnO_2 planes is mediated by the superexchange interaction between localized t_{2g} states, favoring AFM ordering. Consequently, an A-type AFM structure is stabilized at high pressures, as shown in Fig. 4. We note a center of inversion is preserved at the Mn site even in the strained state (tetragonal distortion). Hence, on-site $4p$ - $3d$ mixing remains small and does not change significantly under pressure, consistent with the absence of a preedge feature in the XANES even at the highest pressures (Fig. 1). The shift in the Mn K absorption edge with pressure, totaling ~ 0.85 eV at 23 GPa (Fig. 1) is due to the compression of MnO_6 octahedra and related shortening of multiple scattering pathways, in agreement with Natoli's rule and similar findings in $LaMnO_3$ [34].

Recent theoretical calculations by Nanda and Satpathy [33] predicted that a critical splitting energy $E_{3z^2-r^2} - E_{x^2-y^2} = 0.15$ eV (corresponding to 0.75% strain for MnO_6

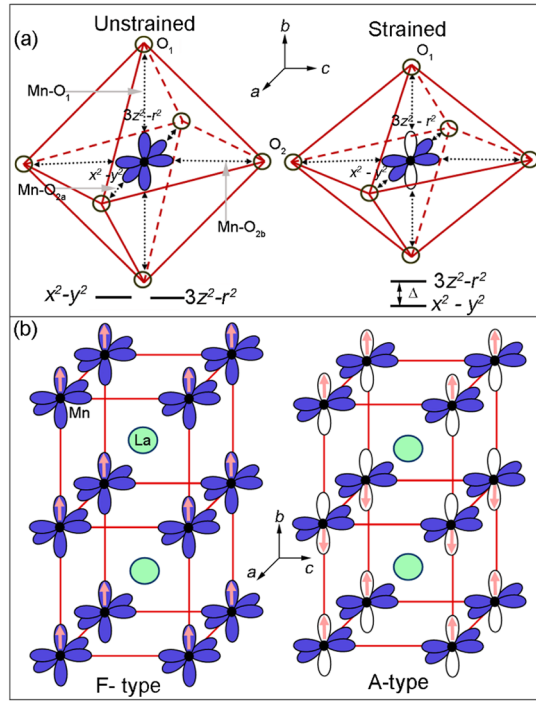


FIG. 4 (color online). (a) MnO_6 octahedra at unstrained and strained conditions. The filled e_g orbitals are occupied by electrons, while the opened e_g orbitals are not occupied by electrons; (b) the structure models for *F*-type and *A*-type magnetic ordering. The arrows inside orbitals indicate the spin direction of d electrons.

octahedra) is needed to trigger a transition from an orbitally disordered *F*-type FM phase to an orbitally ordered *A*-type AFM phase. According to the pressure dependence of strain [dashed line in Fig. 3(b)], the transition is predicted at a pressure of ~ 2 GPa.

Additional evidence in support of this picture is found in recent high-pressure, neutron diffraction experiments where an *A*-type AFM phase was indeed observed to grow within a pure *F*-type FM phase at 1.5 GPa and 150 K, with the volume fraction of the AFM phase increasing with pressure [17]. Within the investigated P - T conditions (0–4 GPa, and 12–298 K), a significant uniaxial anisotropic compression of MnO_6 octahedra along the b axis was also observed [17]. The appearance of an *A*-type antiferromagnetic phase in *F*-type ferromagnetic $La_{0.75}Ca_{0.25}MnO_3$ at such an early compression stage is indicative of a nucleation and growth process, as well as related electronic phase separation, perhaps due to inhomogeneous local strain. Though the nature of the FM-AFM transition could be first order within a single domain, the averaged strain measured in a mixed phase could gradually change with pressure, and it would depend on the growth rate of the AFM phase. The gradual decrease of XMCD is associated with an increase in the volume fraction of the *A*-type AFM phase under pressure. The sudden change in strain and the disappearance of XMCD at ~ 23 GPa rep-

resents the completion of the FM-AFM magnetic transition in the whole sample.

In conclusion, we find a monotonic decrease of the total ferromagnetic moment as a function of pressure combined with an anisotropic distortion of MnO_6 octahedra leading to A-type orbital ordering. The predominant effect of the applied external pressure is to increase the strength of the superexchange interaction relative to the double exchange [8]. As a result, the system tends to increase the number of AFM bonds by decreasing the dimension of the FM region from 3 (*F*-type) to 2 (*A*-type). This directly leads to a strong decrease in hopping integral in one direction, and a concomitant increasing in the population of planar x^2-y^2 orbitals. The resultant nonuniform electron density couples to the lattice via the Jahn-Teller effect causing a strained distortion even under a uniform pressure. This explanation is in agreement with the theoretical prediction of a general sequence of $\text{FM} \rightarrow \text{A-AF} \rightarrow \text{C-AF} \rightarrow \text{G-AF}$ under uniform compression in $\text{La}_{1-x}\text{Sr}_x\text{MnO}_3$ [31].

We are grateful to helpful comments from Dr. Jun Chang. Argonne is supported by the U.S. DOE Contract No. DE-AC02-06CH11357. HPCAT is supported by DOE-BES, DOE-NNSA, NSF, and the W. M. Keck Foundation. APS is supported by DOE-BES, under Contract No. DE-AC02-06CH11357. M. v. V was supported by U.S. DOE DE-FG02-03ER46097. Helium gas loading was performed at GSEACARS.

*yangding@aps.anl.gov

- [1] S. Jin, H. Tiefel, H. McCornack, R. Ramesh, and L. H. Chen, *Science* **264**, 413 (1994).
- [2] C. Zener, *Phys. Rev.* **82**, 403 (1951).
- [3] P. W. Anderson and H. Hasegawa, *Phys. Rev.* **100**, 675 (1955).
- [4] P.-G. de Gennes, *Phys. Rev.* **118**, 141 (1960).
- [5] A. J. Millis, P. B. Littlewood, and B. I. Shraiman, *Phys. Rev. Lett.* **74**, 5144 (1995).
- [6] E. Dagotto, A. Hotta, and A. Moreo, *Phys. Rep.* **344**, 1 (2001).
- [7] C. Cui, T. A. Tyson, Z. Zhong, J. P. Carlo, and Y. Qin *Phys. Rev. B* **67**, 104107 (2003); C. Cui and T. A. Tyson, *Appl. Phys. Lett.* **83**, 2856 (2003); C. Cui, T. A. Tyson, Z. Chen, and Z. Zhong, *Phys. Rev. B* **68**, 214417 (2003); C. Cui and T. A. Tyson, *Appl. Phys. Lett.* **84**, 942 (2004); *Phys. Rev. B* **70**, 094409 (2004).
- [8] A. Sacchetti, P. Postorino, and M. Capone, *New J. Phys.* **8**, 3 (2006).
- [9] E. Duman, M. Acet, E. F. Wassermann, J. P. Itie, F. Baudelet, O. Mathon, and S. Pascarelli, *Phys. Rev. Lett.* **94**, 075502 (2005).
- [10] Y. Ding, D. Haskel, S. G. Ovchinnikov, Y-C. Tseng, Y. S. Orlov, J. C. Lang, and H-k. Mao, *Phys. Rev. Lett.* **100**, 045508 (2008).
- [11] N. Shimatsu, H. Maruyama, N. Kawamura, M. Suzuki, Y. Ohishi, M. Ito, S. Nasu, T. Kawakami, and O. Shimomura, *J. Phys. Soc. Jpn.* **72**, 2372 (2003).

- [12] P. Postorino, A. Congeduti, P. Dore, F. A. Gorelli, A. Sacchetti, L. Ulivi, A. Kumar, and D. D. Sarma, *Phys. Rev. Lett.* **91**, 175501 (2003).
- [13] A. Congeduti, P. Postorino, E. Caramagno, M. Nardone, A. Kumar, and D. D. Sarma, *Phys. Rev. Lett.* **86**, 1251 (2001).
- [14] A. Congeduti, P. Postorino, P. Dore, A. Nucara, S. Lupi, S. Mercone, P. Calvani, A. Kumar, and D. D. Sarma, *Phys. Rev. B* **63**, 184410 (2001).
- [15] C. Meneghini, D. Levy, S. Mobilio, M. Ortolani, M. Nunez-Reguero, A. Kumar, and D. D. Sarma, *Phys. Rev. B* **65**, 012111 (2001).
- [16] D. P. Kozlenko, S. V. Ovsyannikov, V. V. Shchennikov, V. I. Voronin, and B. N. Savenko, *JETP Lett.* **85**, 203 (2007).
- [17] D. P. Kozlenko, S. E. Kichanov, V. I. Voronin, B. N. Savenko, V. P. Glazkov, E. A. Kiseleva, and N. V. Proskurnina, *JETP Lett.* **82**, 447 (2005); D. P. Kozlenko, V. P. Glazkov, R. A. Sadykov, B. N. Savenko, V. I. Voronin, and I. V. Medvedeva, *J. Magn. Magn. Mater.* **258–259**, 290 (2003).
- [18] D. Haskel, Y. C. Tseng, J. C. Lang, and S. Sinogeikin, *Rev. Sci. Instrum.* **78**, 083904 (2007).
- [19] E. E. Rodriguez, Th. Proffen, A. Llobet, J. J. Rhyne, and J. F. Mitchell, *Phys. Rev. B* **71**, 104430 (2005).
- [20] D. D. Ragan, R. Gustavsen, and D. Schiferl, *J. Appl. Phys.* **72**, 5539 (1992).
- [21] A. P. Hammersley, S. O. Svensson, M. Hanfland, A. N. Fitch, and D. Häusermann, *High Press. Res.* **14**, 235 (1996).
- [22] A. C. Larson and R. B. Von Dreele, Los Alamos National Laboratory Report No. LAUR, 86-748, 1994.
- [23] G. Subías, J. García, M. G. Proietti, and J. Blasco, *Phys. Rev. B* **56**, 8183 (1997).
- [24] G. Schütz, W. Wagner, W. Wilhelm, P. Kienle, R. Zeller, R. Frahm, and G. Materlik, *Phys. Rev. Lett.* **58**, 737 (1987).
- [25] H. Sakurai, F. Itoh, H. Maruyama, A. Koizumi, K. Kobayashi, H. Yamazaki, Y. Tanji, and H. Kawata, *J. Phys. Soc. Jpn.* **62**, 459 (1993).
- [26] S. Stahler, G. Schütz, and H. Ebert, *Phys. Rev. B* **47**, 818 (1993).
- [27] I. Harada and A. Kotani, *J. Phys. Soc. Jpn.* **63**, 1285 (1994).
- [28] J. Igarashi and K. Hirai, *Phys. Rev. B* **50**, 17820 (1994).
- [29] C. Brouder, M. Alouani, and K. H. Bennemann, *Phys. Rev. B* **54**, 7334 (1996).
- [30] H. Ebert, in *Spin-Orbit-Influenced Spectroscopies of Magnetic Solids*, edited by H. Ebert and G. Schütz (Springer, Heidelberg, 1996), p. 160.
- [31] Z. Fang, I. V. Solovyev, and K. Terakura, *Phys. Rev. Lett.* **84**, 3169 (2000).
- [32] P. G. Radaelli, G. Iannone, M. Marezio, H. Y. Hwang, S-W. Cheong, J. D. Jorgensen, and D. N. Argyriou, *Phys. Rev. B* **56**, 8265 (1997).
- [33] B. R. K. Nanda and Sashi Satpathy, *Phys. Rev. B* **78**, 054427 (2008).
- [34] C. R. Natoli, *Near Edge Structure III*, Springer Proceedings in Physics Vol. 2 (Springer-Verlag, Berlin, New York, 1984), p. 38; A. Y. Ramos, H. C. N. Tolentino, N. M. Souza-Neto, J. P. Itié, L. Morales, and A. Caneiro, *Phys. Rev. B* **75**, 052103 (2007).